Flow of Power Law Fluids in Tubes of Elliptical Cross Sections

Taha Sochi (Contact: ResearchGate)
London, United Kingdom
Date of Publication: January 23, 2025

Abstract: In this paper we continue our previous investigation about the use of stress function in the flow of generalized Newtonian fluids through conduits of circular and non-circular (or/and multiply connected) cross sections where we inspect the flow of power law fluids in tubes of elliptical cross sections. We derive analytical expressions for the flow velocity profile and for the volumetric flow rate. We also develop numerical algorithms for computing the velocity profile and the volumetric flow rate for this flow where these algorithms produce virtually identical results to the results obtained from the aforementioned analytical expressions. The obtained analytical expressions were tested against the available analytical expressions for the special cases of Newtonian flow in circular tubes, Newtonian flow in elliptical tubes and power law flow in circular tubes and the results were identical. The obtained analytical expressions were also tested for sensible trends, tendencies and correlations and they passed all these tests.[1]

Keywords: Power law fluids, flow in elliptical tubes, non-Newtonian fluids, Newtonian fluids, shear thinning, shear thickening, rheology, fluid mechanics, fluid dynamics, stress function, flow velocity profile, volumetric flow rate, analytical expressions, numerical algorithms.

[1] All symbols and abbreviations are defined in § Nomenclature in the back of this paper.

Contents

1 Introduction

Power law is a popular fluid model that is commonly used in rheology and fluid mechanics to represent time-independent non-Newtonian rheology and fluid flow phenomena in bulk and *in situ*. In fact, power law is the simplest time-independent non-Newtonian fluid model that represents shear thinning and shear thickening (as well as Newtonian as a special case), and this should largely explain its popularity. Accordingly, there is a huge amount of literature on almost all aspects and applications of power law fluid model in rheology, fluid mechanics, mechanical engineering, chemical engineering, biomedical engineering, medical research, and so on (see for instance [1–23]).

However, the flow of power law fluids in conduits of non-circular (or with multiple connectivity) cross sectional geometries are relatively rare (see for instance [1, 24–27]). This is due to the complexity of such flow phenomena due mainly to the geometric complications introduced by non-circular shapes or multiple connectivity where the dependencies of the flow characteristics and attributes become multi dimensional (as opposite to the flow in tubes of circular cross section where these characteristics and attributes depend on a single dimension, i.e. the tube radius).

In two of our previous investigations (see [28, 29]) we proposed using the stress function to develop a rather simple analytical and numerical strategies for obtaining the flow fields and attributes of generalized Newtonian fluid models in tubes of circular and non-circular (or with multiple connectivity) cross sectional geometries. In this paper we return to those investigations where we examine the flow of power law fluids in tubes of elliptical cross sectional geometry using the stress function approach that we proposed in those investigations (particularly in [29]).

In the present investigation we derive two analytical expressions for the flow velocity profile (one in polar coordinates and one in Cartesian coordinates) and another analytical expression for the volumetric flow rate. We also develop numeric algorithms for computing the velocity profile and the volumetric flow rate for this flow where these algorithms produce virtually identical results as those obtained from the aforementioned analytical expressions.

The derived analytical expressions and developed numerical algorithms were tested for certain limiting cases (namely the flow of Newtonian fluids in circular tubes, the flow of Newtonian fluids in elliptical tubes and the flow of power law fluids in circular tubes) and expected trends and correlations (such as the expected shear thinning and shear thickening behaviors and their effects on the variation of flow velocity profile and volumetric flow rate)

where these analytical expressions and numerical algorithms passed all these tests.

Our plan in this paper (following this introduction) is to prepare the scene for this investigation by stating the assumptions and conditions that apply to the fluid, flow and tube (see § 2). We then present the stress-function-based mathematical formulations which lead to the derivation of the aforementioned analytical expressions (see § 3). An outline of the tests and checks that were conducted to partially validate the derived formulae and rule out gross errors is then presented (see § 4). The paper is ended with a list of the main achievements and conclusions of this investigation (see § 5).

2 Setting the Scene

In this investigation we assume a laminar, isothermal, incompressible, rectilinear, steady-state, pressure-driven, fully-developed creeping flow of purely-viscous, time-independent fluids characterized by the power law fluid model which is given by:

$$\tau = k\gamma^n \tag{1}$$

The effects of external body forces, such as gravity, as well as the edge effects at the entry and exit zones of the tube are assumed non-existing or negligible. Dependencies of the attributes of fluid and flow on physical factors like temperature, which are not related to fluid deformation, are also ignored assuming fixed conditions or negligible contribution from these factors (noting that this applies to the physique of tube wall and shape as well). The flow is also assumed to be in purely shear mode with no extensional contributions. Regarding the velocity boundary conditions, a no-slip at the tube wall is assumed and hence a zero velocity condition at the fluid-solid interface is maintained. Regarding the pressure boundary conditions we assume constant time-independent pressure at the inlet and outlet of the tube (where this will be elaborated further next).

As for the type of tube, we use a pipe of elliptical cross sectional shape with semi-major axis a and semi-minor axis b where a uniform pressure drop is imposed along the tube length dimension which defines the flow direction. The pressure is supposed to be constant temporally and spatially at each cross section perpendicular to the flow direction where the pressure is assumed to be a sole function of the axial dimension in the flow direction (i.e. the pressure linearly varies along the axial dimension and hence the pressure gradient as a function of the axial dimension is constant).[2] The pipe is assumed to be straight

[2] In fact, we may add: the flow depends on the pressure gradient (which is determined by the difference between the pressure at the inlet and outlet as well as the tube length) but not on the magnitude of the

with a cross sectional area that is constant in shape and size along the flow axial direction. We also assume rigid mechanical properties of the tube wall and hence the tube wall is not deformable under the considered range of pressure (as well as any other physical conditions such as temperature as hinted earlier). In fact, we should assume that the tube wall and shape are inert in their physical and geometrical properties to all the involved physical conditions and variations of the flow system and its ambient conditions.

3 Method and Formulation

As indicated already, the proposal of the use of stress function is fully explained and justified in [28, 29] and hence we do not repeat. So, all we need to do here is to continue from the final stage that we reached in [29] where we identified the components of the stress function (i.e. the Newtonian stress function which we assume here to be universal) for a number of geometries including the elliptical geometry which is the subject of interest in the present investigation.

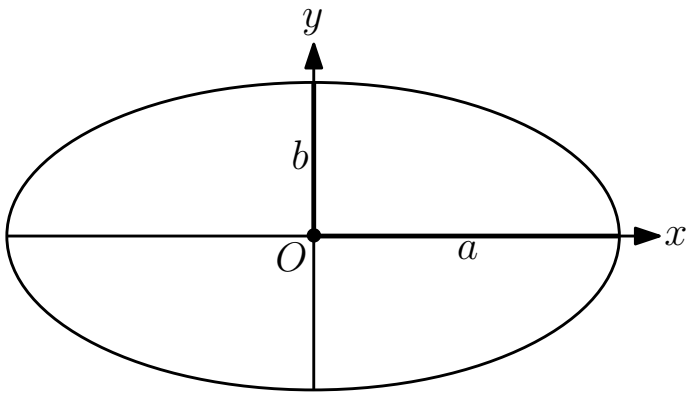

Figure 1: The setting of the elliptical cross section of the tube where a and b represent the semi-major and semi-minor axes and O is the origin of coordinates.

For a tube with an elliptical cross section (centered on the origin of coordinates) of semi-major axis a along the x axis and semi-minor axis b along the y axis (refer to Figure 1) and whose central axis in oriented along the z axis, the components of the stress function are given by:

pressure at the inlet and outlet of the tube (or at any cross section). In other words, the fluid and flow properties (as well as the tube properties) are independent of the magnitude of the applied pressure at the inlet and outlet (or at any cross section).

$$\tau_{xz} = -\frac{\partial p}{\partial z}\frac{b^2 x}{a^2+b^2} \tag{2}$$

$$\tau_{yz} = -\frac{\partial p}{\partial z}\frac{a^2 y}{a^2+b^2} \tag{3}$$

A 2D visualization of the stress function (for an elliptical tube with $a = 3$ and $b = 2$ with a typical pressure gradient) is given in the upper frame of Figure 2, while a 3D visualization of this stress function is given in the lower frame of this Figure.

Now, on the x axis of an elliptical cross section of semi-axes a and b we have $\tau_{yz} = 0$ and hence $\tau = \tau_{xz}$ where τ_{xz} is given by Eq. 2 (but we drop the minus sign as we deal with magnitude). Therefore, the rate of shear strain on the x axis is given by (see Eq. 1):

$$\gamma = \left(\frac{\tau_{xz}}{k}\right)^{1/n} = \left(\frac{\partial p}{\partial z}\frac{b^2 x}{k(a^2+b^2)}\right)^{1/n} = \left(\frac{\partial p}{\partial z}\frac{b^2}{k(a^2+b^2)}\right)^{1/n} x^{1/n} \tag{4}$$

where $0 \le x \le a$. On substituting $\gamma = dv/dx$ in the last equation we get:

$$\frac{dv}{dx} = \left(\frac{\partial p}{\partial z}\frac{b^2}{k(a^2+b^2)}\right)^{1/n} x^{1/n} \tag{5}$$

Now, if v_X symbolizes the fluid velocity at $x = X$ on the x axis (where $0 \le X \le a$) then by integrating the velocity along the x axis (starting from $x = a$, where $v_a = 0$ according to the no-slip at wall condition, and ending at $x = X$) we get:

$$v_X = \int_a^X \frac{dv}{dx}dx \tag{6}$$

$$= \int_a^X \left(\frac{\partial p}{\partial z}\frac{b^2}{k(a^2+b^2)}\right)^{1/n} x^{1/n}\,dx \tag{7}$$

$$= \left(\frac{\partial p}{\partial z}\frac{b^2}{k(a^2+b^2)}\right)^{1/n} \int_a^X x^{1/n}\,dx \tag{8}$$

$$= \left(\frac{\partial p}{\partial z}\frac{b^2}{k(a^2+b^2)}\right)^{1/n} \frac{n}{n+1}\left[x^{(n+1)/n}\right]_a^X \tag{9}$$

$$= \left(\frac{\partial p}{\partial z}\frac{b^2}{k(a^2+b^2)}\right)^{1/n} \frac{n}{n+1}\left[X^{(n+1)/n} - a^{(n+1)/n}\right] \tag{10}$$

Now, a given point of coordinates (x, y) within the ellipse should belong to a given ellipse of the same eccentricity as the original ellipse (i.e. of semi-axes a and b) and with a given semi-major axis X, and hence this point should be on the velocity contour of v_X, i.e. $v(x, y) = v_X$. So, all we need to identify $v(x, y)$ is to identify its corresponding v_X, and this should be easily done by mapping the point (x, y) on the point $(X, 0)$ where we

exploit the basic mathematical formulae and relationships of ellipse, that is:

$$e = \sqrt{1 - (b/a)^2} \tag{11}$$

$$x = r\cos\phi \qquad y = r\sin\phi \tag{12}$$

$$r = \sqrt{x^2 + y^2} \tag{13}$$

$$r = X\sqrt{\frac{1 - e^2}{1 - (e\cos\phi)^2}} \tag{14}$$

$$X = r\sqrt{\frac{1 - (e\cos\phi)^2}{1 - e^2}} \tag{15}$$

On obtaining X from (x, y) as outlined in the above equations we simply substitute from Eq. 15 into Eq. 10 to get our analytical expression of v as a function of (r, ϕ), that is:

$$v(r,\phi) = v_X \tag{16}$$

$$= \left(\frac{\partial p}{\partial z}\frac{b^2}{k(a^2+b^2)}\right)^{1/n}\frac{n}{n+1}\left[\left(r\sqrt{\frac{1-(e\cos\phi)^2}{1-e^2}}\right)^{(n+1)/n} - a^{(n+1)/n}\right] \tag{17}$$

If we substitute $r = \sqrt{x^2 + y^2}$ and $\cos\phi = x/\sqrt{x^2 + y^2}$ in this expression and simplify we get v as a function of (x, y), that is:

$$v(x,y) = \left(\frac{\partial p}{\partial z}\frac{b^2}{k(a^2+b^2)}\right)^{1/n}\frac{n}{n+1}\left[\left(\sqrt{\frac{x^2 - e^2x^2 + y^2}{1-e^2}}\right)^{(n+1)/n} - a^{(n+1)/n}\right] \tag{18}$$

We remark that the minus sign in the v expressions (noting that $X \leq a$) can be interpreted as indicating that the velocity is opposite to the pressure gradient. However, we have no interest in these mathematical technicalities as we are mainly interested in the magnitude of velocity as a function of (r, ϕ) or (x, y) within the elliptical cross section (noting that there is no ambiguity in the physical situation).

Regarding the volumetric flow rate Q we have (where we use the polar version of the velocity profile, i.e. Eq. 17):

$$Q = \left(\frac{\partial p}{\partial z}\frac{b^2}{k(a^2+b^2)}\right)^{1/n}\frac{n}{n+1} \int_{\phi=0}^{\phi=2\pi}\int_{r=0}^{r=b/\sqrt{1-(e\cos\phi)^2}}\left[\left(r\sqrt{\frac{1-(e\cos\phi)^2}{1-e^2}}\right)^{(n+1)/n} - a^{(n+1)/n}\right] r\,dr\,d\phi$$

$$= 4B \int_{\phi=0}^{\phi=\pi/2} \int_{r=0}^{r=b/\sqrt{1-(e\cos\phi)^2}} \left[\left(r\sqrt{\frac{1-(e\cos\phi)^2}{1-e^2}} \right)^{(n+1)/n} r - a^{(n+1)/n} r \right] dr\, d\phi$$

$$= 4B \int_{\phi=0}^{\phi=\pi/2} \int_{r=0}^{r=b/\sqrt{1-(e\cos\phi)^2}} \left[r^{(2n+1)/n} \left(\sqrt{\frac{1-(e\cos\phi)^2}{1-e^2}} \right)^{(n+1)/n} - a^{(n+1)/n} r \right] dr\, d\phi$$

$$= 4B \int_{\phi=0}^{\phi=\pi/2} \left[\frac{n r^{(3n+1)/n}}{(3n+1)} \left(\sqrt{\frac{1-(e\cos\phi)^2}{1-e^2}} \right)^{(n+1)/n} - \frac{a^{(n+1)/n} r^2}{2} \right]_0^{b/\sqrt{1-(e\cos\phi)^2}} d\phi$$

$$= 4B \int_{\phi=0}^{\phi=\pi/2} \left[\frac{n b^{(3n+1)/n} \left(\sqrt{\frac{1-(e\cos\phi)^2}{1-e^2}} \right)^{(n+1)/n}}{(3n+1)\left[\sqrt{1-(e\cos\phi)^2}\right]^{(3n+1)/n}} - \frac{a^{(n+1)/n} b^2}{2\left[1-(e\cos\phi)^2\right]} \right] d\phi$$

$$= 4B \int_{\phi=0}^{\phi=\pi/2} \left[\frac{n b^{(3n+1)/n}}{(3n+1)\left[1-(e\cos\phi)^2\right]} \left(\frac{1}{1-e^2} \right)^{(n+1)/(2n)} - \frac{a^{(n+1)/n} b^2}{2\left[1-(e\cos\phi)^2\right]} \right] d\phi$$

$$= 4B \int_{\phi=0}^{\phi=\pi/2} \left[\frac{n b^{(3n+1)/n}}{(3n+1)\left(1-e^2\right)^{(n+1)/(2n)}} - \frac{a^{(n+1)/n} b^2}{2} \right] \frac{d\phi}{1-(e\cos\phi)^2}$$

$$= 4BC \int_{\phi=0}^{\phi=\pi/2} \frac{d\phi}{1-(e\cos\phi)^2}$$

$$= \frac{4BC}{\sqrt{1-e^2}} \left[\arctan\left(\frac{\tan\phi}{\sqrt{1-e^2}} \right) \right]_0^{\pi/2}$$

$$Q = \frac{4BC}{\sqrt{1-e^2}} \arctan\left(\frac{\tan(\pi/2)}{\sqrt{1-e^2}} \right) \tag{19}$$

where

$$B = \left(\frac{\partial p}{\partial z} \frac{b^2}{k(a^2+b^2)} \right)^{1/n} \frac{n}{n+1} \tag{20}$$

$$C = \frac{n b^{(3n+1)/n}}{(3n+1)\left(1-e^2\right)^{(n+1)/(2n)}} - \frac{a^{(n+1)/n} b^2}{2} \tag{21}$$

It is worth noting that although the tangent function (tan) diverges at $\pi/2$ it is reversed by the inverse tangent function (i.e. arctan). Anyway, as long as we avoid the exact value of $\pi/2$ (which is realized numerically anyway) we can approach $\pi/2$ arbitrarily closely without any problem. In fact, we tested this formula in many cases without encountering any problem. We should also note that the negative sign can be reversed by reversing the difference in C (or taking the absolute value).

Similarly, we have (where we use the Cartesian version of the velocity profile, i.e. Eq.

18):

$$Q = 4\left(\frac{\partial p}{\partial z}\,\frac{b^2}{k(a^2+b^2)}\right)^{1/n}\frac{n}{n+1} \int_{x=0}^{x=a}\int_{y=0}^{y=b\sqrt{1-(x/a)^2}}\left[\left(\sqrt{\frac{x^2-e^2x^2+y^2}{1-e^2}}\right)^{(n+1)/n} - a^{(n+1)/n}\right] dy\,dx \quad (22)$$

However, this integral does not seem to be evaluable analytically, but it can be evaluated numerically (i.e. for specific a, b, k, n and $\partial p/\partial z$). Anyway, Eq. 19 should be sufficient.

4 Tests and Checks

A number of tests and checks on the analytical expressions for the flow velocity profile (i.e. Eqs. 17 and 18) and the volumetric flow rate (i.e. Eq. 19) were conducted to partially validate the derived expressions and exclude gross errors. A sample of these tests and checks are outlined in the following subsections.

4.1 Dimensional Checks

Dimensional inspection of the analytical expressions for the flow velocity profile (i.e. Eqs. 17 and 18) reveals that they have the physical dimension of length over time which is the physical dimension of velocity as it should be. Similarly, dimensional inspection of the analytical expression for the volumetric flow rate (i.e. Eq. 19) reveals that it has the physical dimension of volume over time which is the physical dimension of volumetric flow rate as it should be.

4.2 Velocity Profile Tests

Thorough investigation to the flow velocity profile of the derived formulae (i.e. Eqs. 17 and 18) in the following three special cases (which represent three common types of flow in tubes) was conducted:

1. Circular Newtonian (i.e. Poiseuille): the velocity profile for the flow of Newtonian fluids through a circular tube of radius R is given by (see [30]):

$$v(r) = \frac{R^2 - r^2}{4\mu}\nabla P \quad (23)$$

The results of the derived analytical expressions for the flow velocity profile (i.e. Eqs. 17 and 18 with $n = 1$, $a = b = R$, $k = \mu$ and $\partial p/\partial z = \nabla P$) were compared to the results

of this formula (i.e. Eq. 23) and they were identical. A sample of these comparisons is given in Figure 3.

2. Elliptic Newtonian: the velocity profile for the flow of Newtonian fluids through a tube of elliptical cross section with semi-axes a and b is given by (see [31, 32]):

$$v(x,y) = \frac{a^2 b^2}{2\mu(a^2+b^2)}\left(1 - \frac{x^2}{a^2} - \frac{y^2}{b^2}\right)\nabla P \tag{24}$$

The results of the derived analytical expressions for the flow velocity profile (i.e. Eqs. 17 and 18 with $n = 1$, $k = \mu$, and $\partial p/\partial z = \nabla P$) were compared to the results of this formula (i.e. Eq. 24) and they were identical. A sample of these comparisons is given in Figure 4.

3. Circular power law: the velocity profile for the flow of power law fluids through a circular tube of radius R is given by (see [30]):

$$v(r) = \frac{n}{n+1}\sqrt[n]{\frac{\nabla P}{2k}}\left(R^{1+1/n} - r^{1+1/n}\right) \tag{25}$$

The results of the derived analytical expressions for the flow velocity profile (i.e. Eqs. 17 and 18 with $a = b = R$, $k = \mu$, and $\partial p/\partial z = \nabla P$) were compared to the results of this formula (i.e. Eq. 25) and they were identical. A sample of these comparisons is given in Figure 5.

4.3 Volumetric Flow Rate Tests

Thorough investigation to the volumetric flow rate of the derived formula (i.e. Eq. 19) in the following three special cases (which represent three common types of flow in tubes) was conducted:

1. Circular Newtonian (i.e. Poiseuille): the volumetric flow rate for the flow of Newtonian fluids through a circular tube of radius R is given by (see [30]):

$$Q = \frac{\pi R^4}{8\mu}\nabla P \tag{26}$$

The results of the derived analytical expression for the volumetric flow rate (i.e. Eq. 19 with $n = 1$, $a = b = R$, $k = \mu$, and $\partial p/\partial z = \nabla P$) were compared to the results of this formula (i.e. Eq. 26) and they were identical. A sample of these comparisons is given in Figure 6.

2. Elliptic Newtonian: the volumetric flow rate for the flow of Newtonian fluids through a

tube of elliptical cross section with semi-axes a and b is given by (see [31, 32]):

$$Q = \frac{\pi a^3 b^3}{4\mu(a^2 + b^2)} \nabla P \tag{27}$$

The results of the derived analytical expression for the volumetric flow rate (i.e. Eq. 19 with $n = 1$, $k = \mu$ and $\partial p/\partial z = \nabla P$) were compared to the results of this formula (i.e. Eq. 27) and they were identical. A sample of these comparisons is given in Figure 7.

3. Circular power law: the volumetric flow rate for the flow of power law fluids through a circular tube of radius R is given by (see [30]):

$$Q = \frac{\pi n}{3n + 1} \sqrt[n]{\frac{\nabla P}{2k}} R^{3+1/n} \tag{28}$$

The results of the derived analytical expression for the volumetric flow rate (i.e. Eq. 19 with $a = b = R$, $k = \mu$ and $\partial p/\partial z = \nabla P$) were compared to the results of this formula (i.e. Eq. 28) and they were identical. A sample of these comparisons is given in Figure 8.

4.4 Trends, Tendencies and Correlations

Trends, tendencies and correlations of the derived formulae for the flow velocity profile (i.e. Eqs. 17 and 18) and for the volumetric flow rate (i.e. Eq. 19) were investigated and they were found sensible and inline with expectations. For example:

1. The effect of varying the flow behavior index n on shear thinning and shear thickening (and hence on the flow velocity profile and volumetric flow rate) was investigated and found to be logical and sensible. This also applies to the variation of the viscosity coefficient k. An example of these investigations is given in Figure 9.
2. The effect of varying the tube geometry (such as the tube size and eccentricity) was investigated and found to be logical and sensible.
3. The effect of varying the pressure gradient was investigated and found to be logical and sensible.

4.5 Further Tests

We are not aware of any other theoretical or experimental proposals or results that we can compare with our results in this study. Therefore, we look for other researchers in this field to assess and test our proposals and results theoretically and empirically.

5 Conclusions

We outline in the following points the main achievements and conclusions of the present paper:

1. In this investigation we derived three analytical formulae that represent the flow velocity profile (i.e. Eqs. 17 and 18) and the volumetric flow rate (i.e. Eq. 19) for the flow of power law fluids in tubes of elliptical cross sections.
2. We tested these formulae by developing numerical algorithms corresponding to these formulae and the formulae passed these tests.
3. We tested the convergence of these formulae to three special cases representing three types of flow (i.e. the flow of Newtonian fluids in circular tubes, the flow of Newtonian fluids in elliptical tubes, and the flow of power law fluids in circular tubes) and the formulae passed these tests.
4. We inspected trends, tendencies and correlations indicated by these formulae and the results of all these inspections were sensible and as expected.
5. If there is any doubt about the validity of the proposals and formulae that we presented and derived in this investigation (i.e. mainly the proposal of stress function and Eqs. 17, 18 and 19), there should be no doubt about the value of these proposals and formulae as each one of these three formulae which are derived from the proposal of stress function represents three types of flow (i.e. circular Newtonian, elliptical Newtonian and circular power law) simultaneously, and this condensation of formulation should be very useful theoretically and practically (e.g. in modeling and coding).

References

[1] S. Middleman. Flow of Power Law Fluids in Rectangular Ducts. *Journal of Rheology*, 9(1):83–93, 1965.

[2] R. Christopher; S. Middleman. Power-law flow through a packed tube. *Industrial & Engineering Chemistry Fundamentals*, 4(4):422–426, 1965.

[3] A.H.P. Skelland. *Non-Newtonian Flow and Heat Transfer*. John Wiley & Sons Inc., 1967.

[4] D. Teeuw; F.T. Hesselink. Power-law flow and hydrodynamic behaviour of biopolymer solutions in porous media. *SPE Fifth International Symposium on Oilfield and Geothermal Chemistry, May 28-30, Stanford, California, SPE 8982*, 1980.

[5] R.B. Bird; R.C. Armstrong; O. Hassager. *Dynamics of Polymeric Liquids*, volume 1. John Wiley & Sons, second edition, 1987.

[6] A.V. Shenoy. Darcy-Forchheimer Natural, Forced and Mixed Convection Heat Transfer in Non-Newtonian Power-law Fluid-Saturated Porous Media. *Transport in Porous Media*, 11(3):219–241, 1993.

[7] P.J. Carreau; D. De Kee; R.P. Chhabra. *Rheology of Polymeric Systems*. Hanser Publishers, 1997.

[8] C. Shah; H. Kharabaf; Y.C. Yortsos. Immiscible Displacements Involving Power-Law Fluids in Porous Media. *Proceedings of the Seventh UNITAR International Conference on Heavy Crude and Tar Sands, Beijing, China*, 1998.

[9] R.I. Tanner. *Engineering Rheology*. Oxford University Press, second edition, 2000.

[10] R.B. Bird; W.E. Stewart; E.N. Lightfoot. *Transport Phenomena*. John Wiley & Sons, second edition, 2002.

[11] A. Fadili; P.M.J. Tardy; J.R.A. Pearson. A 3D filtration law for power-law fluids in heterogeneous porous media. *Journal of Non-Newtonian Fluid Mechanics*, 106(2):121–146, 2002.

[12] R. Manica; A.L. de Bortoli. Simulation of Incompressible Non-Newtonian Flows Through Channels with Sudden Expansion using the Power-Law Model. *Tendências em Matemática Aplicada e Computacional*, 4(3):333–340, 2003.

[13] S.P. Sullivan; L.F. Gladden; M.L. Johns. Simulation of power-law fluid flow through porous media using lattice Boltzmann techniques. *Journal of Non-Newtonian Fluid Mechanics*, 133(2–3):91–98, 2006.

[14] B.M. Johnston; P.R. Johnston; S. Corney; D. Kilpatrick. Non-Newtonian blood flow in human right coronary arteries: transient simulations. *Journal of Biomechanics*, 39(6):1116–1128, 2006.

[15] R. Revellin; Fr. Rousset; D. Baud; J. Bonjour. Extension of Murray's law using a non-Newtonian model of blood flow. *Theoretical Biology and Medical Modelling*, 6:1–9, 2009.

[16] T. Sochi. The flow of power-law fluids in axisymmetric corrugated tubes. *Journal of Petroleum Science and Engineering*, 78(3-4):582–585, 2011.

[17] Z.Q. Zhou; J. Peng. Simulation of non-Newtonian (Power-law) fluid flow past a row of square cylinders. *Science China Physics, Mechanics and Astronomy*, 54(4):703–710, 2011.

[18] B. Liu; D. Tang. Non-Newtonian Effects on the Wall Shear Stress of the Blood Flow in Stenotic Right Coronary Arteries. *International Conference on Computational & Experimental Engineering and Sciences*, 17(2):55–60, 2011.

[19] A.S. Wang; D.H. Liang; F. Bech; J.T. Lee; C.K. Zarins; W. Zhou; C.A. Taylor. Validation of a Power Law Model in Upper Extremity Vessels: Potential Application in Ultrasound Bleed Detection. *Ultrasound in Medicine & Biology*, 38(4):692–701, 2012.

[20] M.M. Molla; M.C. Paul. LES of non-Newtonian physiological blood flow in a model of arterial stenosis. *Medical Engineering & Physics*, 34(8):1079–1087, 2012.

[21] T. Sochi. The Flow of Newtonian and power law fluids in elastic tubes. *International Journal of Non-Linear Mechanics*, 67:245–250, 2014.

[22] T. Sochi. The flow of power law fluids in elastic networks and porous media. *Computer Methods in Biomechanics and Biomedical Engineering*, 2015.

[23] C. Lambride; A. Syrakos; G.C. Georgiou. Entrance length estimates for flows of power-law fluids in pipes and channels. *Journal of Non-Newtonian Fluid Mechanics*, 317:105056, 2023.

[24] R.S. Schechter. On the steady flow of a non-Newtonian fluid in cylinder ducts. *AIChE Journal*, 7(3):445–448, 1961.

[25] C. Miller. Predicting Non-Newtonian Flow Behavior in Ducts of Unusual Cross Section. *Industrial & Engineering Chemistry Fundamentals*, 11(4):524–528, 1972.

[26] M. Escudier; P. Oliveira; F. Pinho; S. Smith. Fully developed laminar flow of non-Newtonian liquids through annuli: comparison of numerical calculations with experiments. *Experiments in Fluids*, 33(1):101–111, 2002.

[27] Y.S. Muzychka; J. Edge. Laminar Non-Newtonian Fluid Flow in Noncircular Ducts and Microchannels. *Journal of Fluids Engineering*, 130(111201):1–7, 2008.

[28] T. Sochi. Using the stress function in the flow of generalized Newtonian fluids through pipes and slits. 2015. arXiv:1503.07600.

[29] T. Sochi. Using the stress function in the flow of generalized Newtonian fluids through conduits with non-circular or multiply connected cross sections. 2015. arXiv:1509.01648.

[30] T. Sochi. Using the Euler-Lagrange variational principle to obtain flow relations for generalized Newtonian fluids. *Rheologica Acta*, 53(1):15–22, 2014.

[31] F.M. White. *Viscous Fluid Flow*. McGraw Hill Inc., second edition, 1991.

[32] J. Lekner. Viscous flow through pipes of various cross-sections. *European Journal of Physics*, 28(3):521–527, 2007.

Nomenclature

2D, 3D	two dimensional, three dimensional
a, b	semi-major and semi-minor axes of ellipse (m)
e	eccentricity of ellipse ( )
Eq., Eqs.	Equation, Equations
k	viscosity coefficient in the power law model (Pa.s^n)
n	flow behavior index in the power law model ( )
p	pressure (Pa)
Q	volumetric flow rate (m^3.s^{-1})
r	radius (m)
R	pipe radius (m)
r, ϕ	polar coordinates (m,)
v	fluid velocity (m.s^{-1})
v_X	fluid velocity value on the coordinates $x = X$ and $y = 0$ (m.s^{-1})
$v(r, \phi)$	fluid velocity as a function of polar coordinates (m.s^{-1})
$v(x, y)$	fluid velocity as a function of Cartesian coordinates (m.s^{-1})
x, y, z	coordinate variables (usually spatial coordinates)
∇P	pressure gradient (Pa.m^{-1})
γ	rate of shear strain (s^{-1})
μ	Newtonian viscosity (Pa.s)
τ	shear stress (Pa)
τ_{xz}, τ_{yz}	shear stress components (Pa)

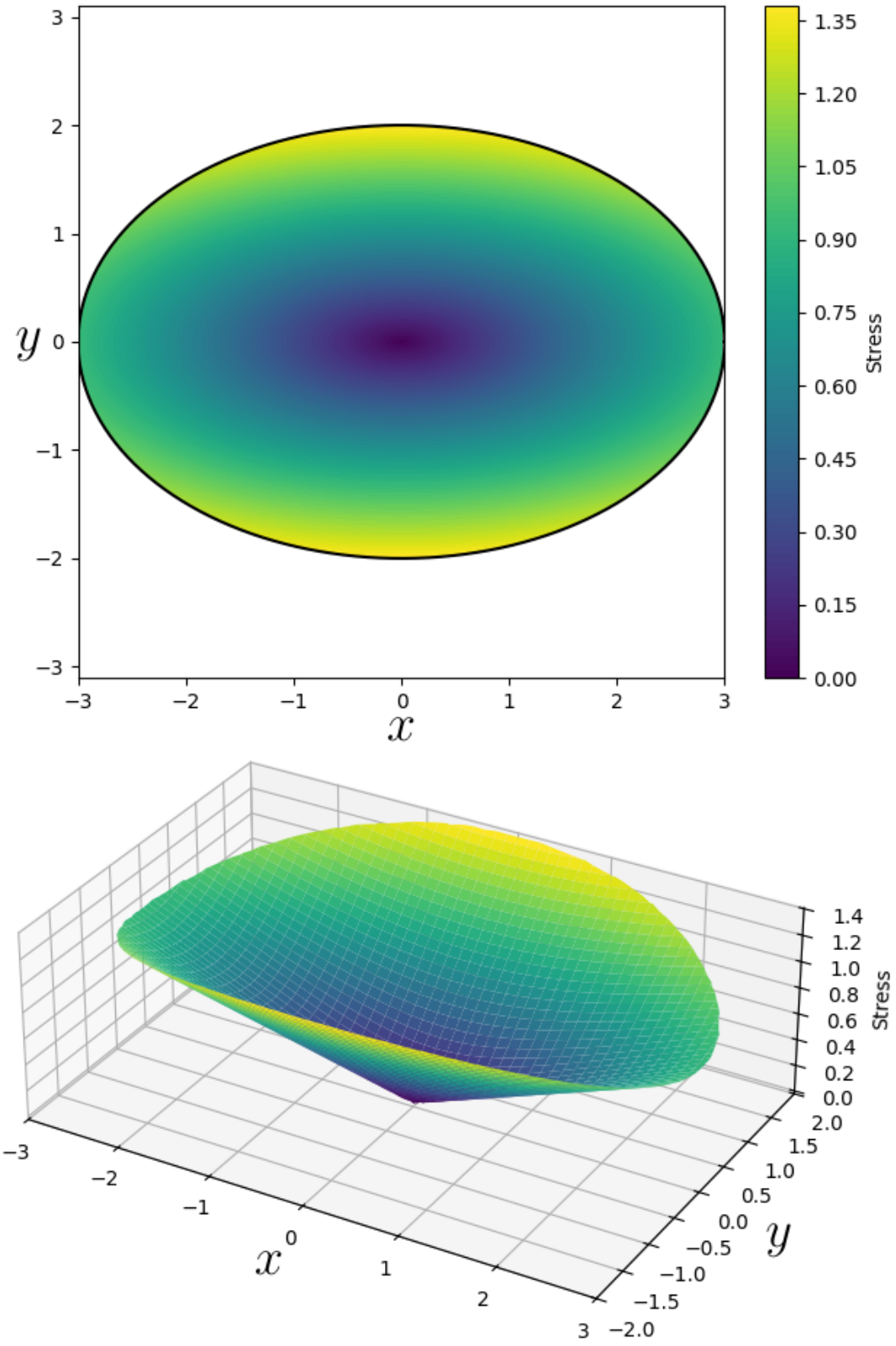

Figure 2: 2D and 3D graphic illustrations of the stress function for an elliptical tube with $a = 3$ and $b = 2$ with a typical pressure gradient.

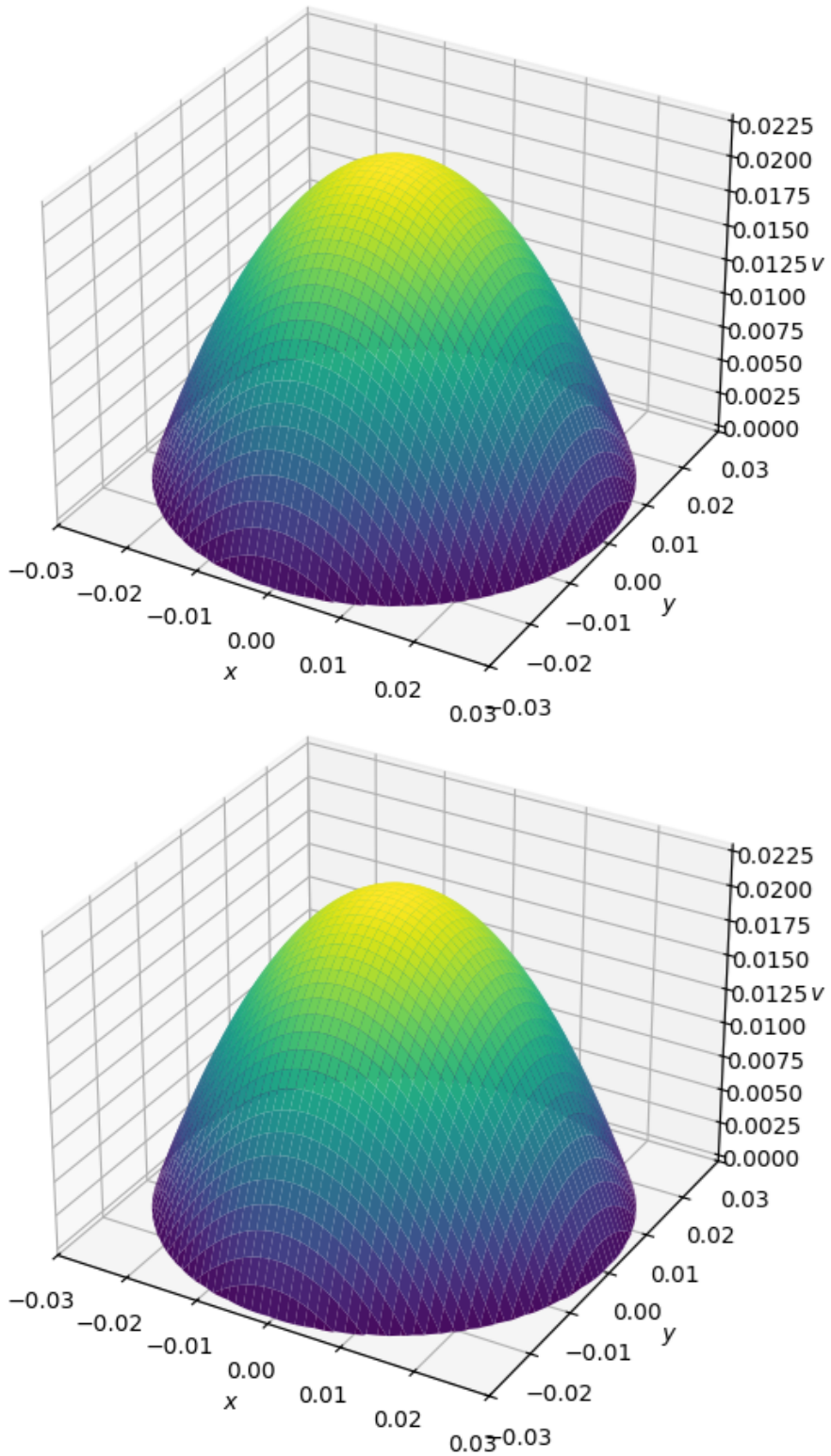

Figure 3: A 3D plot of the velocity profile for the Newtonian flow in circular tube as given by Eq. 23 (upper frame) and the power law flow in elliptical tube as given by Eq. 18 (lower frame) with $n = 1$, $a = b = R = 0.03$, $k = \mu = 0.1$ and $\partial p/\partial z = \nabla P = 10$. As we see, the two plots are identical.

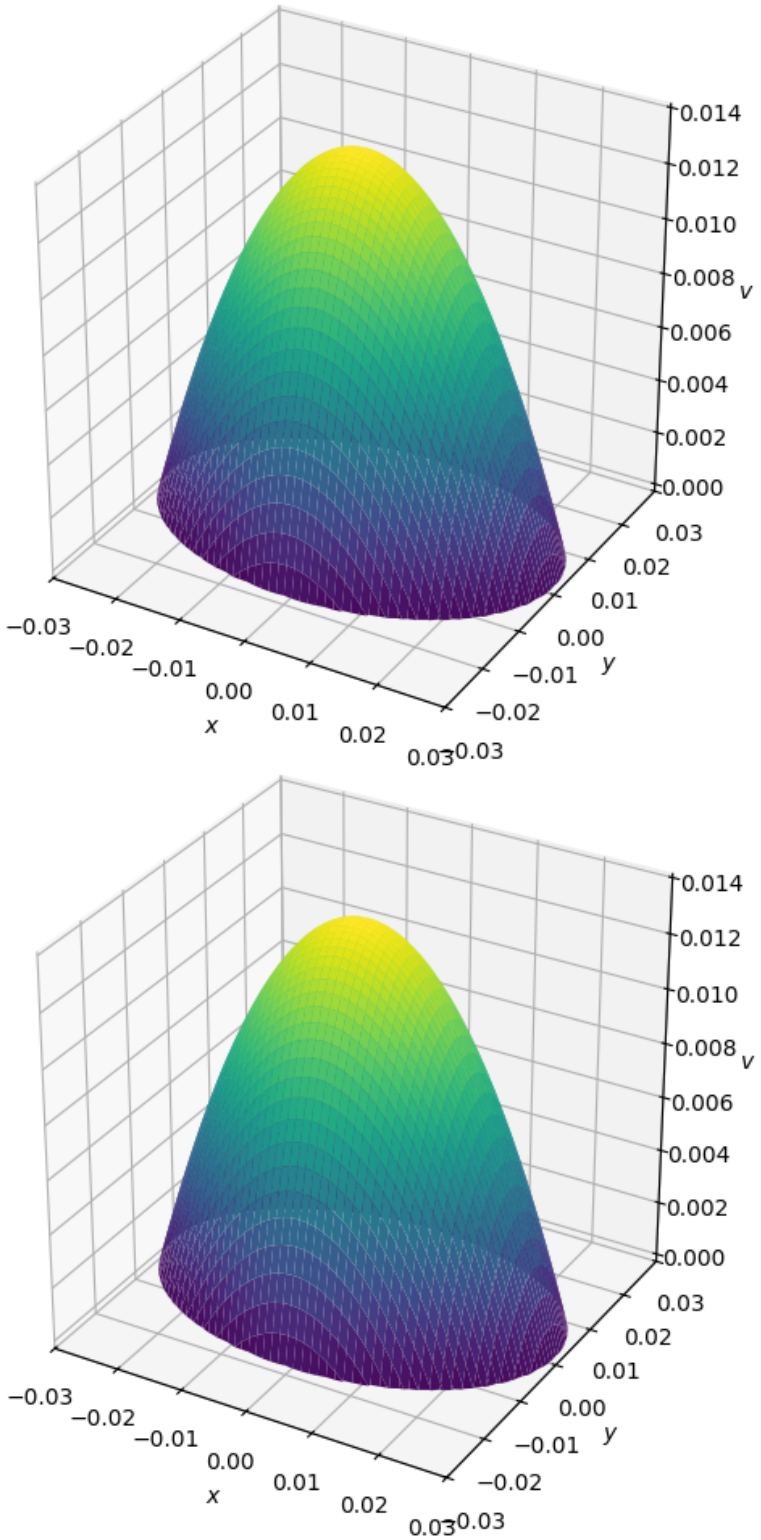

Figure 4: A 3D plot of the velocity profile for the Newtonian flow in elliptical tube as given by Eq. 24 (upper frame) and the power law flow in elliptical tube as given by Eq. 18 (lower frame) with $n = 1$, $a = 0.03$, $b = 0.02$, $k = \mu = 0.1$ and $\partial p/\partial z = \nabla P = 10$. As we see, the two plots are identical.

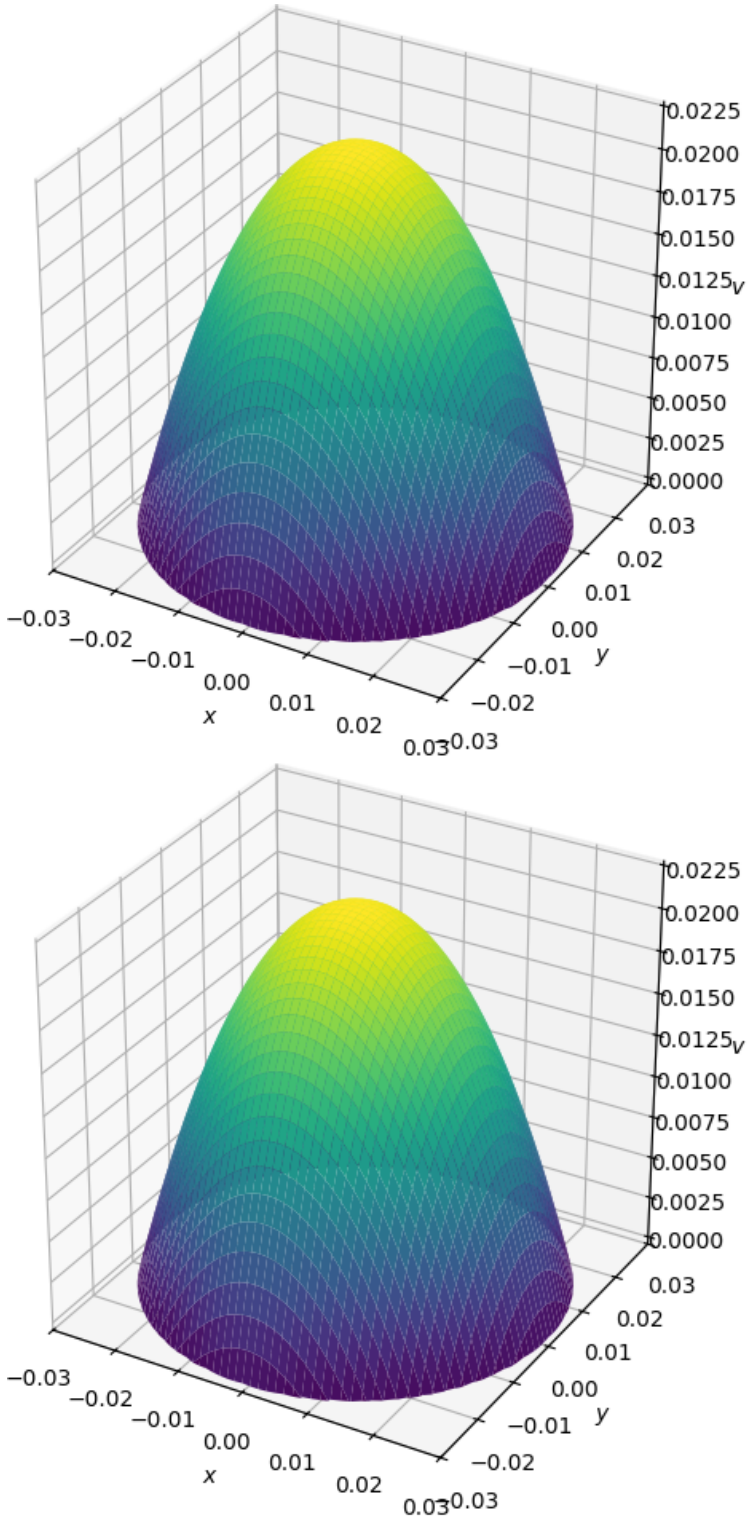

Figure 5: A 3D plot of the velocity profile for the power law flow in circular tube as given by Eq. 25 (upper frame) and the power law flow in elliptical tube as given by Eq. 18 (lower frame) with $n = 0.89$, $a = b = R = 0.03$, $k = 0.1$ and $\partial p/\partial z = \nabla P = 10$. As we see, the two plots are identical.

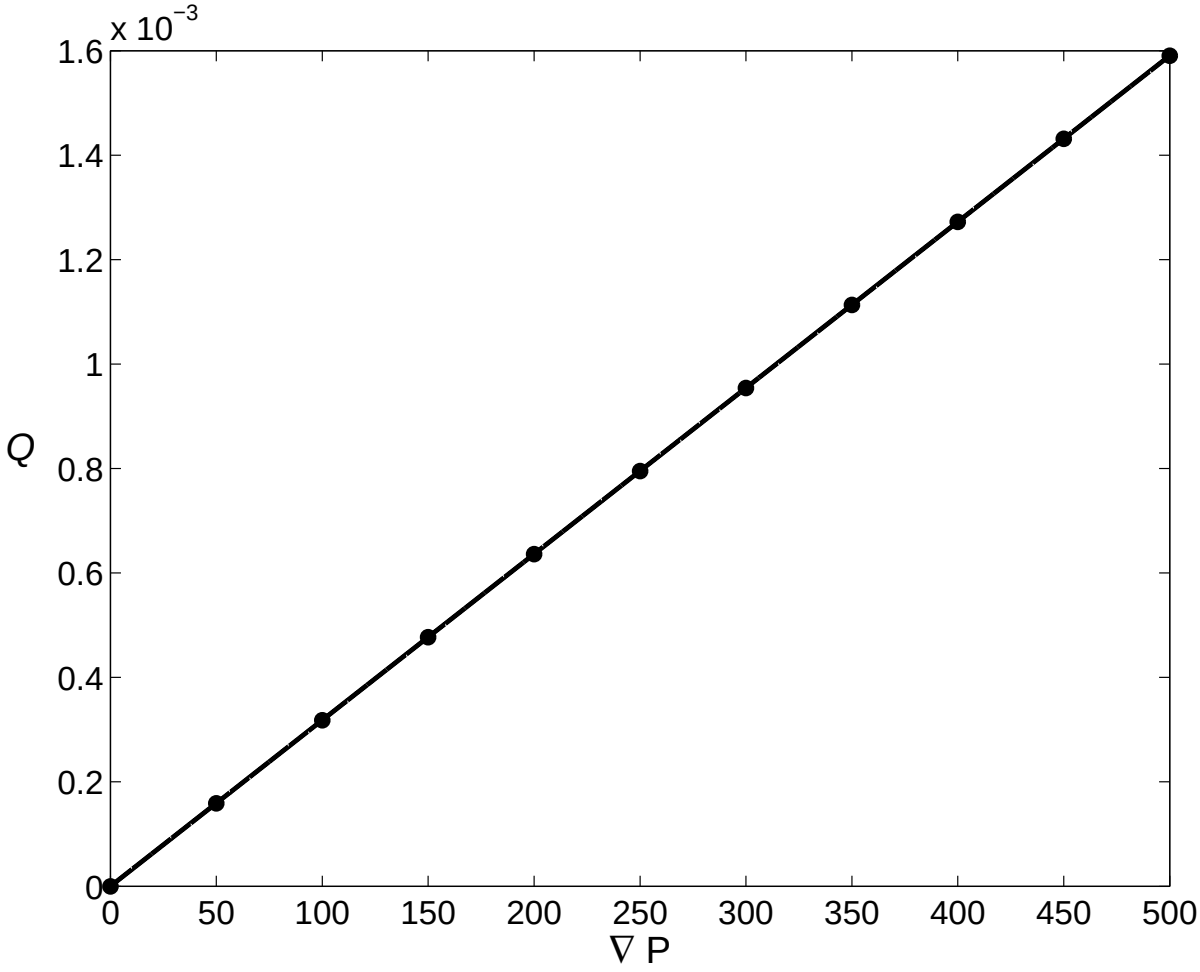

Figure 6: A plot of the volumetric flow rate for the Newtonian flow in circular tube as given by Eq. 26 (continuous line) and the power law flow in elliptical tube as given by Eq. 19 (circles) with $n = 1$, $a = b = R = 0.03$, $k = \mu = 0.1$ and $\partial p/\partial z = \nabla P$.

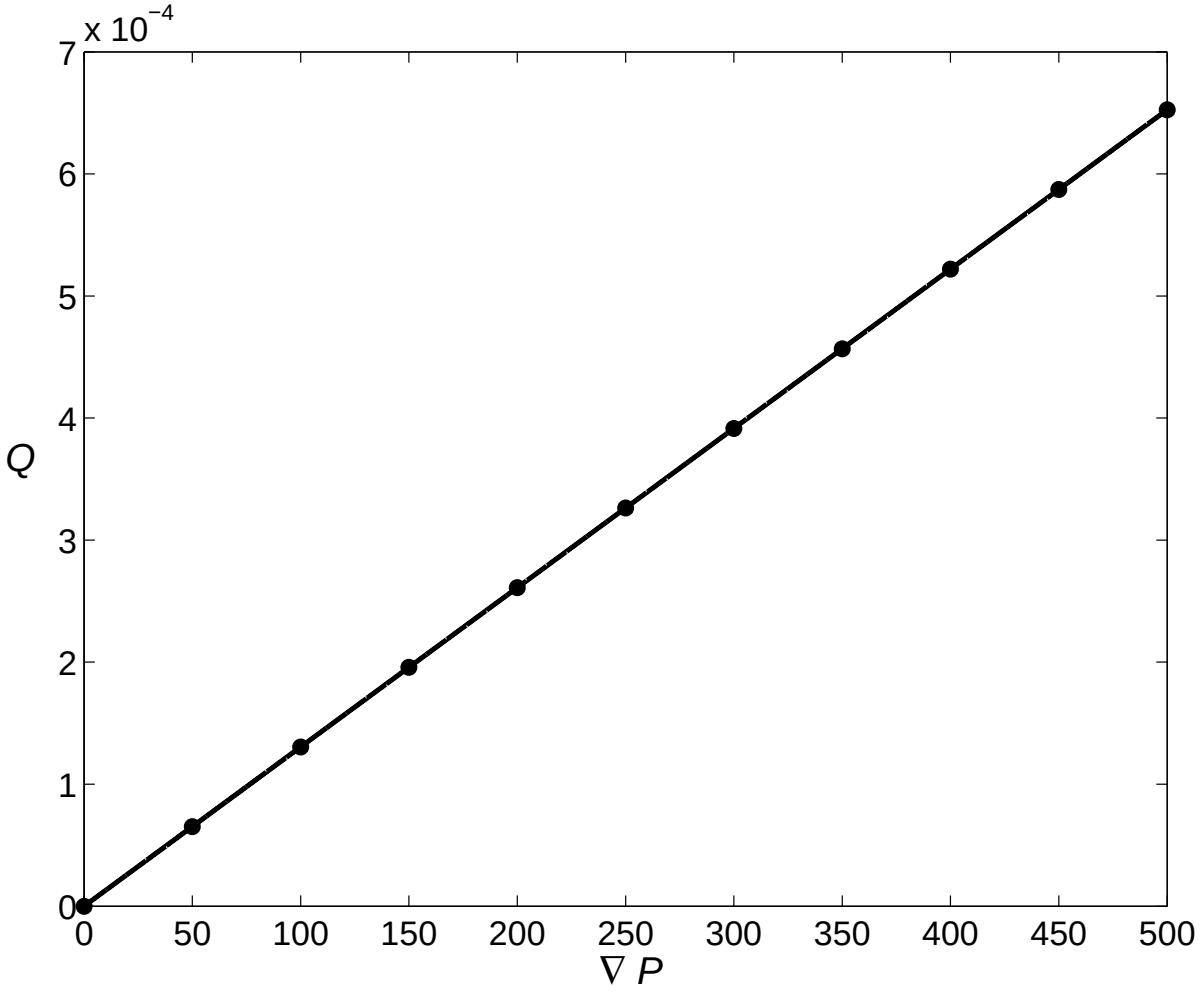

Figure 7: A plot of the volumetric flow rate for the Newtonian flow in elliptical tube as given by Eq. 27 (continuous line) and the power law flow in elliptical tube as given by Eq. 19 (circles) with $n = 1$, $a = 0.03$, $b = 0.02$, $k = \mu = 0.1$ and $\partial p/\partial z = \nabla P$.

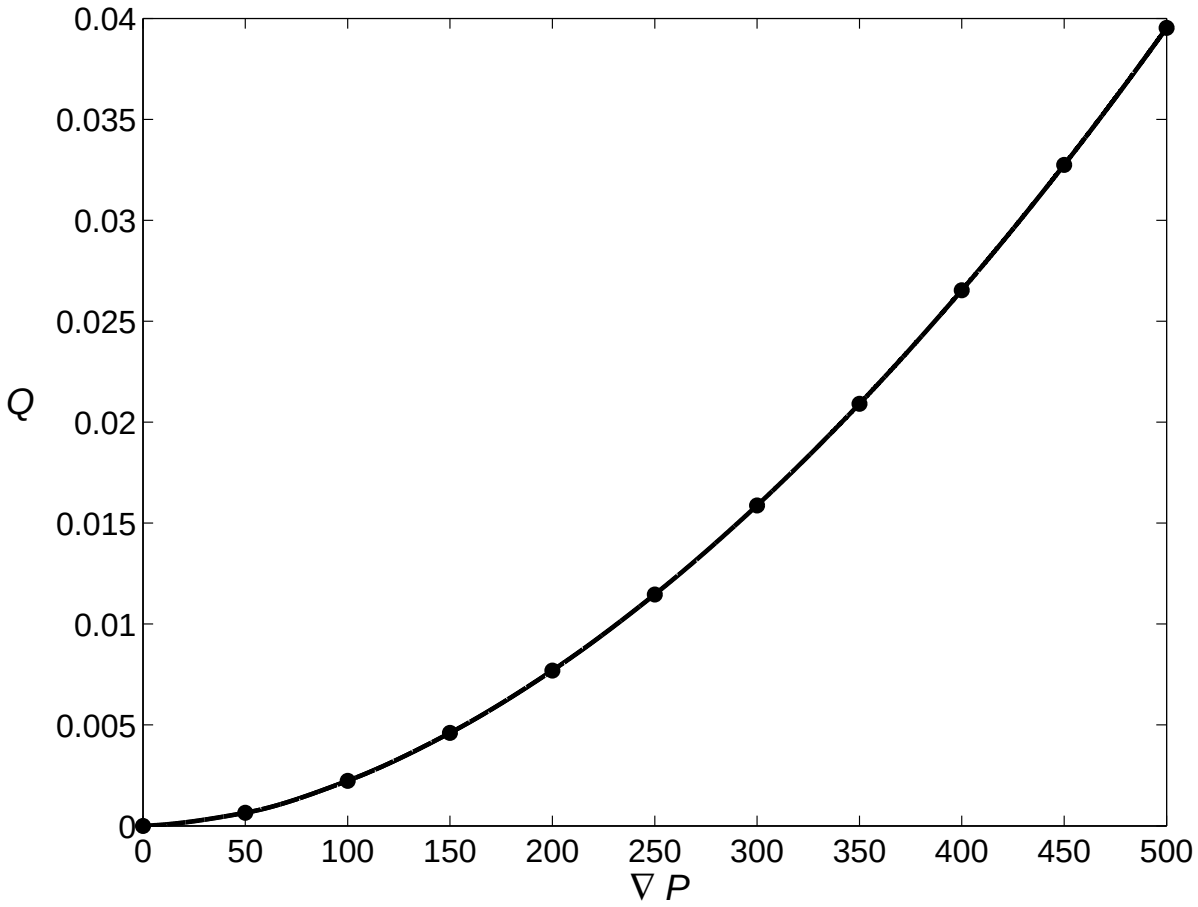

Figure 8: A plot of the volumetric flow rate for the power law flow in circular tube as given by Eq. 28 (continuous line) and the power law flow in elliptical tube as given by Eq. 19 (circles) with $n = 0.56$, $a = b = R = 0.03$, $k = 0.1$ and $\partial p/\partial z = \nabla P$.

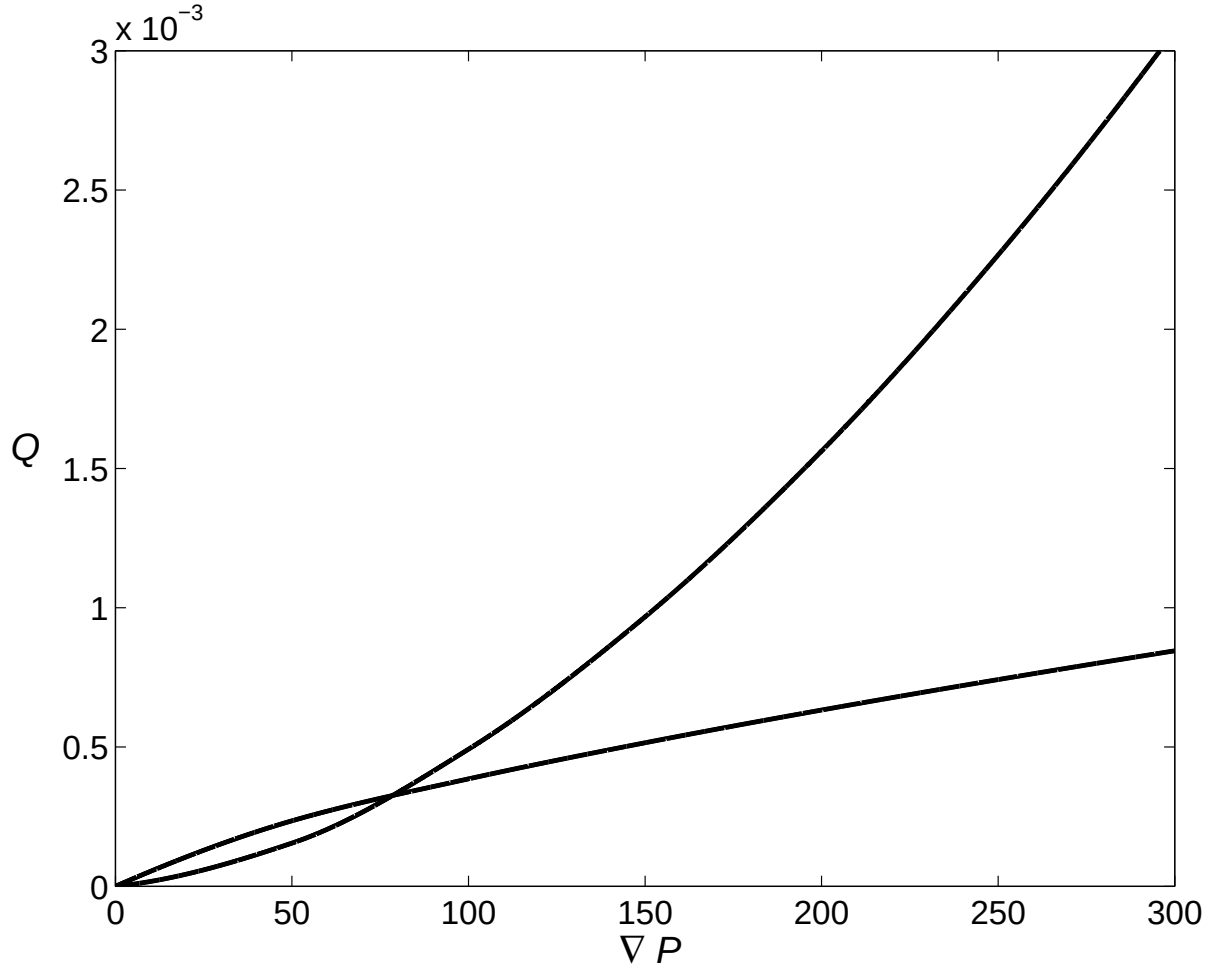

Figure 9: Shear thinning (with $n = 0.6$ and $k = 0.1$) and shear thickening (with $n = 1.4$ and $k = 0.01$) for the power law flow in an elliptical tube with $a = 0.03$ and $b = 0.02$ (using Eq. 19).